# Cluster Formation and Particle-Induced Instability in Gas-Solid Flows Predicted by the DSMC Method*

Toshitsugu TANAKA**, Shigeru YONEMURA**,
Ken KIRIBAYASHI*** and Yutaka TSUJI**

A numerical simulation is performed for a dispersed gas-solid flow in a vertical channel. Flow of the solid phase is obtained by calculating individual particle motions, i.e. by the Lagrangian method, while the gas flow is obtained by solving the equations of inviscid fluid. The Direct Simulation Monte Carlo (DSMC) method is used to take account of particle-to-particle collisions. Attention is paid to the case of low gas velocities and high solid loading, for which the solid phase strongly affects the gas flow field. Therefore the flow fields of gas and solid are determined simultaneously taking the interaction between both phases into consideration. It is found that the flow becomes unstable and inhomogeneous as the gas velocity decreases and the solid loading increases. Furthermore, effects of parameters such as the channel width and physical properties of particles on the instability and cluster formation are investigated.

***Key Words***: Multiphase Flow, Gas-Solid Flow, Circulating Fluidized Bed, Cluster, DSMC Method, Numerical Simulation

## 1. Introduction

The flow pattern of gas-solid flow in a vertical pipe or a duct depends on the flow conditions. Many studies on such flows have concerned industrial applications such as pneumatic conveyers and fluidized beds, and there are many papers in which the change of flow pattern is mentioned (for example Yerushalmi et al.[1]). When the gas velocity is large and the solid loading is small, the flow is stable and particles are distributed homogeneously. By contrast, the flow becomes unstable and inhomogeneous at low gas velocity and high solid loading.

Such an unstable flow pattern is observed in fast fluidized beds and in dense-phase pneumatic conveyers. This kind of instability is induced by the existence of particles and has significant effects on transport phenomena between gas and solid phases, which are important in many industrial applications. Therefore it is necessary to specify the critical conditions, and determine the structure of unstable flows. Many diagrams of flow patterns have been suggested, since the relation between flow patterns and operation conditions is needed for designing facilities (for example Grace[2]). However such diagrams only give rough estimates.

One distinguishing feature of this kind of unstable flow is the existence of clusters, which are remarkably dense regions in the flow. Horio and Kuroki[3] observed the spatial structure of clusters in a circulating fluidized bed. They found that the typical shape of clusters is a paraboloid facing downward. They also measured the size of clusters.

Numerical simulation is a promising method to study these phenomena, because the presence of particles does not make the flow fields less accessible, and it is easy to change parameters. Papers dealing with such dispersed unstable flows are rather few, as far as we know. Tsuo and Gidaspow[4] calculated flow patterns in circulating fluidized beds. They used the two-fluid model in which the solid phase is modeled as a viscous fluid with constant effective viscosity, and

* Received 13th February, 1995. Japanese original: Trans. Jpn. Soc. Mech. Eng., Vol. 59, No. 566, B (1993), pp. 2982-2989. (Received 14th December, 1992)

** Department of Mechanical Engineering for Industrial Machinery, Osaka University, 2-1 Yamada-oka, Suita, Osaka 565, Japan

*** Sumitomo Metal Industries, Ltd., 1850 Minato, Wakayama 640, Japan

predicted unstable flows with clusters, as observed in practice. However, the assumption of a continuum becomes invalid when the mean free path of particles is not sufficiently small compared with spatial scales of changes. The Lagrangian method, in which trajectories of individual particles are calculated, is more suitable for such flows. Another advantage of this method is that particle-to-wall and particle-to-particle interactions can be taken into account based on the physical properties of the materials concerned.

In the present work, flow instability induced by particles in the case of low gas velocities were studied numerically. Furthermore the structure of clusters, and the dependence of such structures on flow conditions are investigated. Two-way coupling between both phases was accounted for. To model particle-to-particle collisions the direct simulation Monte Carlo (DSMC) method, first proposed by Bird[5] for solving the Boltzmann equation of rarefied gas flows, was applied when calculating particle motion.

## 2. Governing Equations and Numerical Methods

### 2.1 Particle motion

**2.1.1 Treatment of particle motion** The flows studied in the present paper are two-dimensional. This means that macroscopic flows of both phases are two-dimensional, but individual particle motion is not restricted to two-dimensional as in the case of molecules in a two-dimensional gas flow. Only locally averaged properties of particles are assumed to be two-dimensional.

**2.1.2 DSMC method** When inertia forces dominate fluid drag, the particle-to-particle interaction in a dispersed gas-solid flow is well described by the impulsive equations of motion in which collisions with another particle or wall are assumed to occur instantaneously. Therefore the motion of the solid phase is similar to that of molecules in rarefied gas except that the kinetic energy of fluctuating particle motion tends to decay due to the inelastic and frictional aspects of collision.

The DSMC method has already been applied to calculate particle motion in gas-solid flows by Kitron et al.[6], Shimomizuki et al. and Tanaka et al.[8] Tanaka et al. applied the DSMC method to fully developed flows in a vertical pipe and obtained results which agree well with those predicted by the deterministic method (Tanaka and Tsuji[9]).

The outline of the DSMC method is as follows.

(1) Each simulated particle represents a large number of "physical" particles.

(2) The time step is small compared with the mean free time of particles, and thus particle-to-particle collisions are uncoupled from free particle motion.

(3) The flow field is divided into small cells in which the change in flow properties is small, within which particles are allowed to collide by a Monte Carlo method.

According to the DSMC method the calculation of particle motion was carried out by repeating the following procedure:

(1) First, the motions of all simulated particles in the time interval $\Delta t$ are calculated using the equations of motion without regard for particle-to-particle collisions. If the calculated path of a particle crosses a solid wall, the velocity is replaced with the post-rebound velocity.

(2) Second, particle-to-particle collision during the time interval $\Delta t$ is examined by means of the Monte Carlo procedure described in the next section. The collision partner and geometry of collision are also chosen by the Monte Carlo method.

(3) If a particle collides with another particle, the post-collision velocities of the colliding pair are calculated using the impulsive equations. The particle velocities are replaced by the post-collision velocities, without changing the particle positions.

Several schemes to examine whether a particle collides with another particle in a time step have been proposed. The modified Nanbu method, which was proposed by Illner and Neunzert[10], was used in the present calculations. Let us consider the collision probability of simulated particle $i$ in a time step $\Delta t$. The collision probability is given by

$$P_i=\sum_{j=1}^{N}P_{ij}, \qquad (1)$$

where $N$ is the number of simulated particles in the cell and $P_{ij}$ the probability of collision between simulated particles $i$ and $j$ contained in the cell in the time step $\Delta t$.

When $P_{ij}$ is evaluated, it must be noted that each simulated particle represents many physical particles. $P_{ij}$ is not a collision probability between single particle $i$ and single particle $j$ but that for a physical particle in a field over which physical particles represented by simulated particles $i$ and $j$ are distributed uniformly. Assuming the particles are spheres which have a uniform diameter $d$, $P_{ij}$ is given by

$$P_{ij}=\frac{n}{N}\pi d^2 g_{ij}\Delta t, \qquad (2)$$

where $n$ is the number density of the real flow at the corresponding position, and $g_{ij}$ is the magnitude of relative velocity between the particles. The ratio $n/N$ is determined from the imposed inlet conditions using Eq. (17), (section 2. 1. 5).

In the modified Nanbu method, the occurrence of particle-to-particle collision and the collision partner

are determined according to a random number $R_{ND}$ obtained from a uniform distribution which ranges from zero to unity. A "candidate" collision partner $k$ is selected first via the equation

$$k=[[R_{ND}N]]+1, \quad (3)$$

where $[[R_{ND}N]]$ is the integer part of $R_{ND}N$. Particle $i$ is then assumed to collide with particle $k$ during the previous time step if

$$R>\frac{k}{N}-P_{ik}. \quad (4)$$

In this procedure, $P_{ij}$ for any particle combination in a cell must not exceed $1/N$. This condition is satisfied by choosing an appropriate time step, since $P_{ij}$ is proportional to $\Delta t$ as shown in Eq.(2).

If particle $i$ collides with particle $k$, the velocity of particle $i$ (though not that of $k$) is replaced by the velocity after the collision according to the impulsive equations in section 2. 1. 4, for which the relative position of collision is also given by random numbers.

**2.1.3 Equations of particle motion** Particles are assumed to be rigid spheres whose diameter, mass and other physical properties are uniform. The equation of translational motion of particles is

$$m\frac{d\boldsymbol{v}}{dt}=\boldsymbol{F}_f+m\boldsymbol{g}_G, \quad (5)$$

where $m$ is the mass of a particle, $\boldsymbol{v}$ is particle velocity, $\boldsymbol{g}_G$ is the gravitational acceleration, and $\boldsymbol{F}_f$ is the fluid force assumed to be given by

$$\boldsymbol{F}_f=\frac{1}{2}\rho_f|\boldsymbol{u}_R|A\left(C_D\boldsymbol{u}_R+C_{LR}\frac{\boldsymbol{u}_R\times\boldsymbol{\omega}_R}{|\boldsymbol{\omega}_R|}\right)+\boldsymbol{f}_{LG}, \quad (6)$$

where $A$ is the projected area of a particle, $\rho_f$ is fluid density, $\boldsymbol{u}_R$ is gas velocity relative to the particle, and $\boldsymbol{\omega}_R$ is the rotational velocity of the particle relative to the fluid;

$$\boldsymbol{\omega}_R=\boldsymbol{\omega}-\frac{1}{2}\nabla\times\boldsymbol{u}, \quad (7)$$

where $\boldsymbol{\omega}$ is the rotational velocity of the particle.

The first term on the right-hand side of Eq.(6) represents the drag force, the second term, the Magnus lift force, and $\boldsymbol{f}_{LG}$, the lift force due to velocity gradient.

The standard drag coefficient for a sphere in a uniform flow was used as $C_D$ (Morsi and Alexander[11]). The following expression was assumed for $C_L$ based on experiments at moderate and high Reynolds number (Maccoll[12], Davis[13], Barkla and Auchterlonie[14], Tanaka et al.[15]).

$$C_L=\min\left[0.5,\ 0.25\frac{d\omega}{|\boldsymbol{u}_R|}\right] \quad (8)$$

where $\min[a, b]$ is the minimum value of $a$ and $b$.

For the lift force $F_{LG}$ due to velocity gradient, Saffman's[16] theoretical result was used. Only the $y$ component of $\boldsymbol{F}_{LG}$ was considered here.

$$\boldsymbol{F}_{LGy}=1.62u_{Rz}d^2\sqrt{\rho_f\mu}\frac{du_{Rz}/dy}{\sqrt{|du_{Rz}/dy|}} \quad (9)$$

where $u_{Rz}$ is the $z$ component of $\boldsymbol{u}_R$.

The equation of rotational motion of a particle is expressed as

$$I\frac{d\boldsymbol{\omega}}{dt}=-C_T\frac{1}{2}\rho\frac{d^5}{2}|\boldsymbol{\omega}_R|\boldsymbol{\omega}_R, \quad (10)$$

where $I$ is the moment of particle inertia. The right-hand side of Eq.(10) is the viscous torque against particle rotation, which was theoretically obtained by Dennis et al.[17] and Takagi[18]. $C_T$ is the nondimensional coefficient which is a function of $Re_R=|\boldsymbol{\omega}_R|d^2/(4\nu)$.

**2.1.4 Collision** It is assumed that the relaxation time of particles due to fluid forces is long compared with the duration of particle interaction. Consequently fluid forces due to interactions between particles are neglected. When a particle collides with another particle or a wall, the post-collision velocities are calculated using the equations of impulsive motion as follows,

$$\boldsymbol{v}^*=\boldsymbol{v}+\boldsymbol{J}/m, \quad (11)$$

$$\boldsymbol{\omega}^*=\boldsymbol{\omega}+\frac{d}{2I}\boldsymbol{n}\times\boldsymbol{J}, \quad (12)$$

where $\boldsymbol{n}$ is the unit normal vector directed outwards from the particle at the contact point, and $\boldsymbol{J}$ is the impulsive force exerted on the particle. Post-collision quantities are indicated by an asterisk.

The following assumptions are introduced to calculate the impulsive force $\boldsymbol{J}$.

(1) Particles are spherical, and particle deformation negligible.

(2) The coefficient of restitution is constant.

(3) The tangential impulsive force during the slip motion is given by Coulomb's friction law.

(4) Slip between particles does not occur again after the initial slip.

According to these assumptions $\boldsymbol{J}$ is given as follows (Tsuji et al.[19], Tanaka and Tsuji[9]).

$$\boldsymbol{J}=J_n\boldsymbol{n}+J_t\boldsymbol{t} \quad (13)$$

$$J_n=(1+e)M\boldsymbol{n}\cdot\boldsymbol{g} \quad (14)$$

$$J_t=\min\left[-\mu_F J_n,\ \frac{2}{7}M|\boldsymbol{g}_F|\right] \quad (15)$$

In the above equation, $\boldsymbol{t}$ is the tangential unit vector directed toward $\boldsymbol{g}_F$ which is the slip velocity of the collision partner, $e$ is the coefficient of restitution, $\mu_F$ is the coefficient of kinetic friction, and $M=m/2$ for collision with another particle, $M=m$ for collision against a wall.

**2.1.5 Conditions at inlet and outlet boundary** The configuration of the calculation domain is shown schematically in Fig. 1. This configuration is similar to that used by Tsuo and Gidaspow[4]. A constant number of simulated particles are introduced at every time step through the inlet boundary. Initial positions of simulated particles are given by random numbers

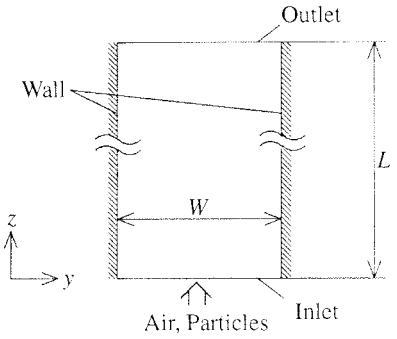


Fig. 1 Configuration of the calculation domain

so that the particle distribution is on average uniform at the inlet. An isotropic fluctuation component of magnitude $v_I'$ is added to the mean inlet velocity of particles, $V_I$. No initial rotational velocity is given to particles.

The solid mass flux at the inlet $Q_p$ was imposed as a parameter of the calculation. Assuming that the calculation region has unit depth, $Q_p$ is related to the rate of introduction of simulated particles by:

$$Q_p=\alpha\frac{mN_{IN}}{W\Delta t}, \tag{16}$$

where $N_{IN}$ is the number of simulated particles introduced at each time step, $W$ is the width of the channel, and $\alpha$ is the ratio of "physical" particle concentration to that of simulated particles. When the solid volume fraction and the momentum exchange between both phases are evaluated as in the preceding section, contributions of simulated particles are multiplied by a weighting coefficient. The ratio $n/N$ in Eq.(2) is related to $\alpha$ via:

$$\frac{n}{N}=\frac{\alpha}{\Delta y_p\Delta z_p}, \tag{17}$$

where $\Delta y_p$ and $\Delta z_p$ are sizes of cells for the calculation of particle collision.

### 2.2 Calculation of fluid flow

The fluid is assumed to be incompressible and inviscid except for the force on particles. The fluid flow field is described using "local mean variables" which are defined as locally averaged values in the volume occupied by the fluid (Anderson and Jackson[20]). The spatial scale of local averaging is larger than that of particles but small compared with that of change of macroscopic flow properties. The equation of continuity and the equation of motion used here are as follows;

$$\frac{\partial\varepsilon}{\partial t}+\nabla\cdot(\varepsilon\boldsymbol{u})=0, \tag{18}$$

$$\varepsilon\frac{D\boldsymbol{u}}{Dt}=-\frac{\varepsilon}{\rho_f}\nabla p+\frac{\boldsymbol{F}_p}{\rho_f}, \tag{19}$$

where $\varepsilon$ is the void fraction, $p$, pressure, and $\boldsymbol{F}_p$, the force exerted on the fluid by particles per unit volume of fluid.

Table 1 Calculation conditions

| | |
|---|---|
| $\Delta t$ (s) | $5\times10^{-4}$ |
| $L$ (m) | 2 |
| $W$ (mm) | 80, 300 |
| $\rho_f$ (kg/m$^3$) | 1.205 |
| $\nu$ (m$^2$/s) | $1.515\times10^{-5}$ |
| $d$ (mm) | 0.5 |
| $\rho_p$ (kg/m$^3$) | 2620 |
| $e_p$ | 1, 0.94, 0.5 |
| $e_w$ | 0.94 |
| $\mu_{Fp}$ | 0, 0.28 |
| $\mu_{Fw}$ | 0.28 |
| $\lvert\boldsymbol{V}_I\rvert$ (m/s) | 0.4 |
| $v_I'$ (m/s) | 0.2 |

These equations were solved by the SIMPLE scheme (Patankar[21]). The flow region was divided into rectangular cells of dimensions $\Delta y_f\times\Delta z_f$. $\varepsilon$ is given explicitly by

$$\varepsilon=1-\frac{\alpha N_f V_p}{\Delta y_f\Delta z_f}, \tag{20}$$

where $N_f$ is the number of simulated particles contained in the fluid calculation cell, and $V_p$, the volume of a particle. $\boldsymbol{F}_p$ is the reaction of fluid forces acting on particles:

$$\boldsymbol{F}_p=-\frac{\alpha}{\Delta y_f\Delta z_f}\sum_{i=1}^{N_f}\boldsymbol{F}_{fi}. \tag{21}$$

## 3. Results and Discussion

### 3.1 Conditions of simulation

The principal conditions are shown in Table 1. The conditions are basically similar to those used by Tsuo and Gidaspow[4]. The physical properties of the gas were chosen to be those of air at atmospheric pressure and room temperature. The terminal velocity of the particles in such a gas is 3.7 m/s. The calculation region is divided into $20\times100$ rectangular cells for both phases. $N_{IN}$ is 25 for $U<8$ m/s, and 50 for $U\geq8$ m/s. The total number of simulated particles in the developed flow ranged from fifty thousand to one hundred and twenty thousand. Preliminary calculations were made for larger cell sizes and smaller numbers of simulated particles, but no significant difference was observed.

### 3.2 Unstable flows

The change of flow pattern due to change in superficial gas velocity is shown in Fig. 2. The vertical scale of the channel is compressed in these figures, and similar scaling is used in the other figures. When the superficial gas velocity is large or the mean solid mass flux is small, the flow is stable and the particle concentration has a nearly homogeneous distribution. In such conditions the effect of particles on the gas flow field is negligible. Consequently the distributions of particle velocity are nearly flat across the channel.

In the case of $U=5$ m/s and $Q_p=25$ kg/m$^2$s the

flow becomes inhomogeneous and unstable. Several particle clusters in which solid volume fraction is extremely large are formed near the wall. These particle clusters substantially affect the gas flow. Gas velocity and particle velocity are reduced in particle clusters and in their wakes.

Figure 3 shows the variation in distributions of solid volume fraction with time. It is observed that nonuniformities appear at some distance from the inlet and develop into clusters. In the region in which clusters are formed the flow shows unstable behavior in space and time. Various phenomena involving clusters are observed in these figures. Some clusters increase in density, while others become sparse and finally vanish. Furthermore it is observed that some clusters grow by coalescence. When the density of a cluster becomes large, it can move downward along the wall.

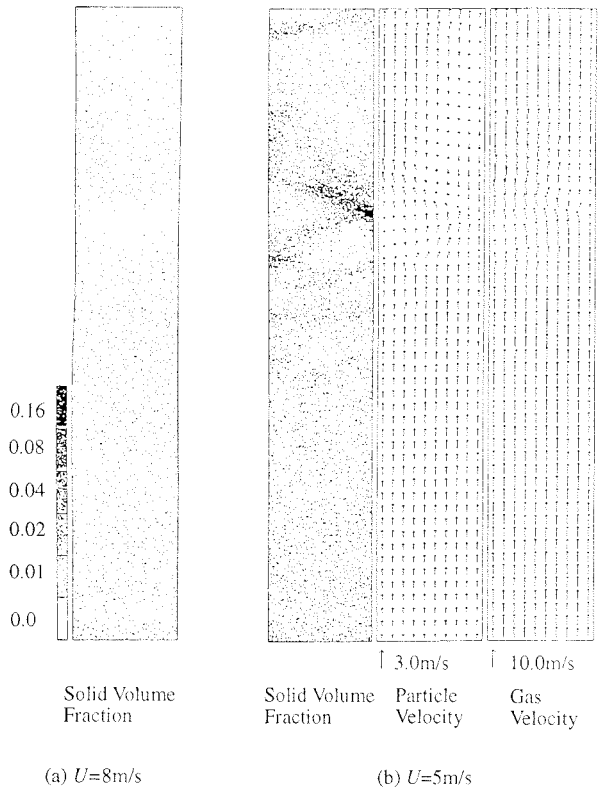


Fig. 2 Effects of superficial gas velocity on flow pattern ($W$=80 mm, $Q_p$=25 kg/m$^2$s, $e_p$=0.94, $\mu_{Fp}$=0.28)

Tsuo and Gidaspow[4] performed a numerical simulation similar to the present one using the two-fluid model. The present results qualitatively agree with their results. For example, clusters tend to form along the side walls also in their simulations. However, there is a quantitative difference. Cluster population in the present simulation is larger than that in their simulation.

Figure 4 shows the relation between the superficial gas velocity and the RMS of solid concentration fluctuation in the fully developed flow region of time and space. It can be seen that flows rapidly become unstable as $U$ approaches 5 m/s from above.

### 3.3 Structure of clusters

Figure 5 shows a flow pattern obtained in the case of $W$=300 mm. In contrast with the case of $W$=80 mm, clusters are formed not only along the walls but also in the central part of the channel. A close-up of a typical V-shaped cluster formed in the central part of the channel is also shown in Fig. 5.

Similar clusters were observed in the experiments by Horio and Kuroki[3], who visualized the structure of clusters in a circulating fluidized bed using the laser sheet technique. They found that the average shape of a cluster in a vertical cross section is a parabola, which is very similar to the present result, and that the three-dimensional structure of such a parabolic

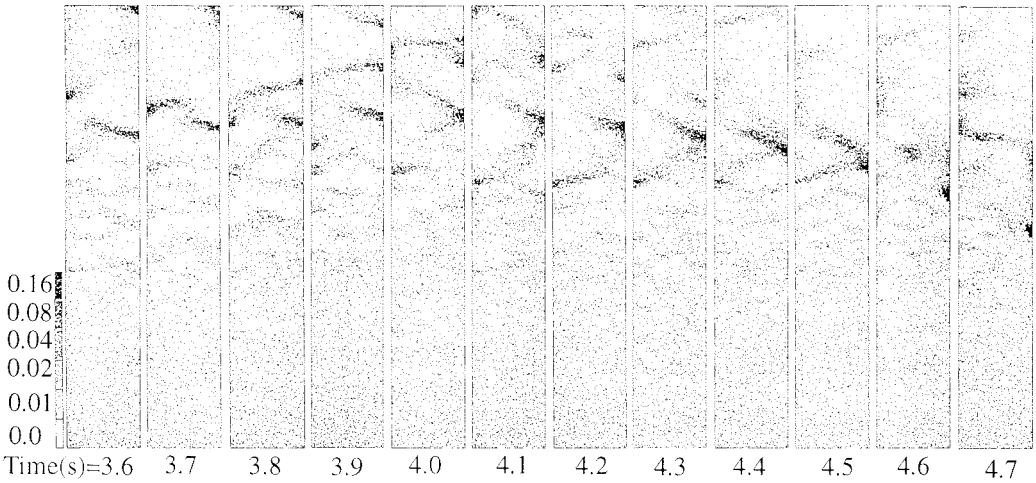


Fig. 3 Variation in distributions of solid volume fraction with time ($W$=80 mm, $U$=5 m/s, $Q_p$=25 kg/m$^2$s, $e_p$=0.94, $\mu_{Fp}$=0.28)

cluster is a paraboloid.

The scale of the close-up is not compressed. Gas velocity is reduced in particle clusters and in their wakes. Velocities of the particles there are correspondingly reduced so that particles are supplied to the clusters both from above and below. On the other hand a cluster discharges particles from its "tail". A cluster grows or disperses according to the balance of supply and discharge.

### 3.4 Effects of inelasticity and friction on cluster formation

As shown in the preceding discussion, growth of nonuniformity and cluster formation are important for investigating unstable flows. It is known that particle clusters can be formed by inelastic collisions even without fluid effect (Shida and Kawai[22]). This type of cluster formation is caused by the dissipation in kinetic energy through particle-to-particle collisions. Therefore the effects of inelasticity and friction on cluster formation were studied.

Some results are shown in Fig. 6, and the effects on the RMS of solid concentration fluctuation are

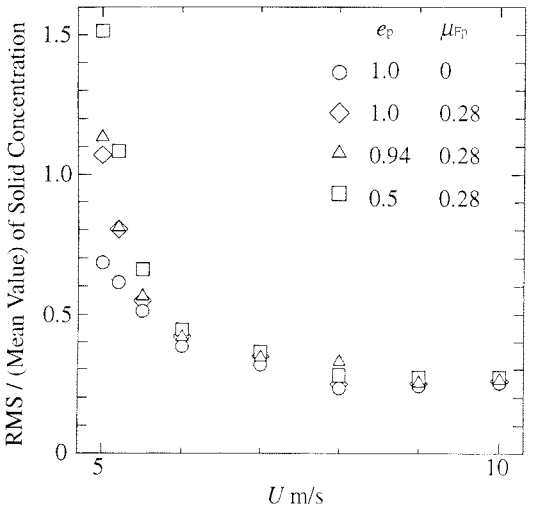


Fig. 4 Relation between superficial gas velocity and concentration fluctuation
($W$=80 mm, $Q_p$=25 kg/m²s)

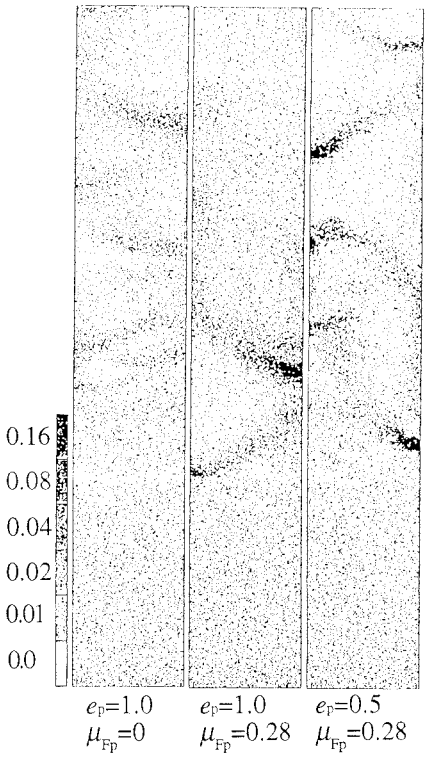


Fig. 6 Effects of inelasticity and friction on cluster formation
($W$=80 mm, $U$=5 m/s, $Q_p$=25 kg/m²s)

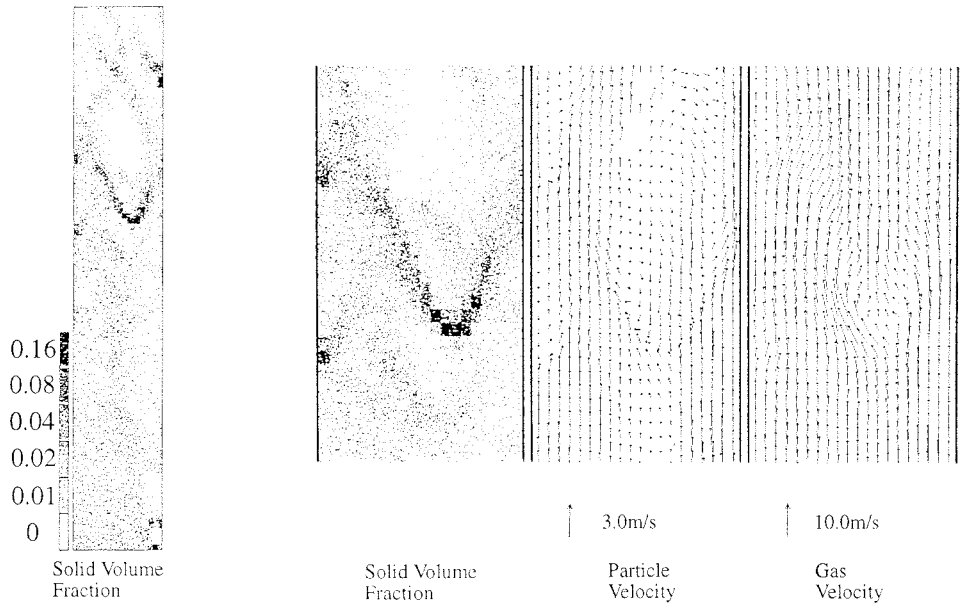


Fig. 5 Flow around a cluster
($W$=300 mm, $U$=5 m/s, $Q_p$=25 kg/m²s, $e_p$=0.94, $\mu_{Fp}$=0.28)

shown in Fig. 4. The coefficient of friction and the coefficient of restitution between particles and wall are constant for these results (see Table 1). In the case of $e_p=1$ and $\mu_{Fp}=0$, kinetic energy does not dissipate through particle-to-particle collisions. Even in this case, the flow becomes unstable, but the growth of clusters is suppressed in comparison with other cases. The results for $e_p=1$ and $\mu_{Fp}=0.28$ show that clusters develop due to friction. From these results it can be seen that the inelasticity and the friction of particle-to-particle collision largely affect the growth of clusters.

## 4. Conclusion

Unstable phenomena and cluster formation of dispersed gas-solid flows were investigated by numerical simulation. The results are summarized as follows.

(1) The flow becomes unstable and inhomogeneous when the superficial gas velocity is low and the solid mass flux is large. The process of growth, coalescence and disappearance of particle clusters was observed.

(2) The pattern of cluster formation is affected by the channel width. When the channel width is small clusters are formed only along the wall. In the case of a wide channel, clusters are formed not only along the walls but also in the central part of the channel.

(3) In the case of a wide channel, a V-shaped cluster, which was observed in the previous experiments, was formed in the central part of the channel.

(4) Flow instability and cluster formation are promoted by inelasticity and friction of particle-to-particle collisions.

## References


(1) Yerushalmi, J., Cankurt, N.T., Geldert, D. and Liss, B., Flow Regimes in Vertical Gas-Solid Contact System, AIChE Symp. Ser., Vol. 74, No. 176 (1978), p. 1.

(2) Grace, J. R., Contacting Modes and Behaviour Classification of Gas-Solid and Other Two-Phase Suspensions, Canadian J. Chem. Eng., Vol. 64 (1986), p. 353.

(3) Horio, M. and Kuroki, H., Three-Dimensional Flow Visualization of Dilute Dispersed Solids in Bubbling and Circulating Fluidized Beds, Chem. Eng. Sci., Vol. 49, No. 15 (1994), p. 2413.

(4) Tsuo, Y.P. and Gidaspow, D., Computation of Flow Patterns in Circulating Fluidized Beds, AIChE J., Vol. 36, No. 6 (1990), p. 885.

(5) Bird, G.A., Molecular Gas Dynamics, (1976), Oxford Univ. Press.

(6) Kitron, A., Elperin, T. and Tamir, A., Monte Carlo Simulation of Gas-Solids Suspension Flows in Impinging Streams Reactors, Int. J. Multiphase Flow, Vol. 16, No. 1 (1990), p. 1.

(7) Shimomizuki, N., Adachi, T., Tanaka, T. and Tsuji, Y., Numerical Analysis of Particle Dynamics in a Bend of a Rectangular Duct by the Direct Simulation Monte Carlo Method, Gas Solid Flows 1993, ASME/FED, Vol. 166 (1993), p. 145.

(8) Tanaka, T., Kiribayashi, K. and Tsuji, Y., Monte Carlo Simulation of Gas-Solid Flow in Vertical Pipe or Channel, Proc. Int. Conf. on Multiphase Flows'91-Tsukuba, Tsukuba, Vol. 2 (1991), p. 439.

(9) Tanaka, T. and Tsuji, Y., Numerical Simulation of Gas-Solid Two-Phase Flow in a Vertical Pipe : On the Effect of Inter Particle Collision, Gas-Solid Flows 1991, ASME/FED, Vol. 121 (1991), p. 123.

(10) Illner, R. and Neunzert, H., On simulation methods for the Boltzmann equation, Transport Theory and Statistical Physics, Vol. 16 (1987), p. 141.

(11) Morsi, S. A. and Alexander, A. J., An Investigation of Particle Trajectories in Two-Phase Flow System, J. Fluid Mech., Vol. 55, Part 2 (1972), p. 193.

(12) Maccoll, J. W., Aerodynamics of a Spinning Sphere, J. Roy. Aero. Sci., Vol. 32 (1928), p. 777.

(13) Davis, J. M., The Aerodynamics of Golf Balls, J. Appl. Phys., Vol. 20, No. 9 (1949), p. 821.

(14) Barkla, H. M. and Auchterlonie, L. J., The Magnus or Robins Effect on Rotation Spheres, J. Fluid Mech., Vol. 47, Part 3 (1971), p. 437.

(15) Tanaka, T., Yamagata, K. and Tsuji, Y., Experiment of Fluid Forces on a Rotating Sphere and Spheroid, Proc. Second KSME JSME Fluids Engineering Conf., Seoul, Vol. 1 (1990), p. 366.

(16) Saffman, P. G., The Lift on a Small Sphere in a Slow Shear Flow, J. Fluid Mech., Vol. 22, Part 2 (1965), p. 385; Vol. 31 (1968), p. 624.

(17) Dennis, S. C. R., Singh, S. N. and Ingham, D. B., The Steady Flow due to a Rotating Sphere at Low and Moderate Reynolds Number, J. Fluid Mech., Vol. 101 (1980), p. 257.

(18) Takagi, H., Viscous Flow Induced by Slow Rotation of a Sphere, J. Phys. Soc. Japan, Vol. 42 (1977), p. 319.

(19) Tsuji, Y., Morikawa, Y., Tanaka, T., Nakatsukasa, N. and Nakatani, M., Numerical Simulation of Gas-Solid Two-Phase Flow in a Two-Dimensional Horizontal Channel, Int. J. Multiphase Flow, Vol. 13, No. 5 (1987), p. 671.

(20) Anderson, T. B. and Jackson, R., A Fluid Mechanical Description of Fluidized Beds, I&EC Fundamentals, (1967), p. 527.

(21) Patankar, S. V., Numerical Heat Transfer and Fluid Flow, Hemisphere Publishing Corporation, (1980)

(22) Shida, K. and Kawai, T., Cluster Formation by Inelastic Collision in One-dimensional Space, Physica A, Vol. 159 (1989), p. 145.